

Alkoxysilylation of Ti-MWW lamellar precursors into interlayer pore-expanded titanosilicates†

Lingling Wang,^{ab} Yong Wang,^a Yueming Liu,^{*a} Haihong Wu,^a Xiaohong Li,^a Mingyuan He^a and Peng Wu^{*a}

Received 3rd June 2009, Accepted 3rd September 2009

First published as an Advance Article on the web 24th September 2009

DOI: 10.1039/b910886f

Silylation of Ti-MWW lamellar precursor and subsequent calcination constructed an interlayer expanded structure, leading to novel titanosilicates with large pores. The silylating agents suitable for pore expansion were diethoxydimethylsilane, trimethylethoxysilane and triethoxymethylsilane containing methyl groups, which inhibited the intermolecular condensation of silanes effectively. In contrast to well-known 3D Ti-MWW with only medium pores of 10-membered rings, the silylation led to new crystalline structures with more open pores by *ca.* 2.5 Å, as evidenced by the shift of layer-related diffractions to the lower-angle region in XRD patterns and the enlarged interlayer pores in HRTEM images. The interlayer expanded Ti-MWW was prepared readily from the corresponding hydrothermally synthesized precursors with a wide range of Ti contents (Si/Ti = 20–100). In addition, the pore expansion by silylation was realized under mild acid conditions with 0.1 M HNO₃. The interlayer expanded Ti-MWW exhibited 3–7 times higher turnover number than 3D Ti-MWW in the oxidation of cyclohexene with H₂O₂.

Introduction

The high reactivity of the oxirane ring makes epoxides industrially important organic intermediates for producing polyurethanes, surfactants, epoxy adhesives, corrosion-protecting reagents, and additives, *etc.*¹ Conventional methods for epoxide synthesis are facing drawbacks such as the use of hazardous halogen reagents, co-production of salts with low value, discharge of a large quantity of wastewater, and severe corrosion of apparatus. Environmentally benign methods are thus required urgently. It is well known that crystalline titanosilicates are highly active and selective catalysts for the production of oxygenated derivatives through the oxidation of hydrocarbons and alcohols, and the ammoximation of ketones with H₂O₂ as an oxidant, in which water is the sole byproduct.^{2–8} The representative titanosilicate is TS-1 with the MFI structure first reported two decades ago.² Extensive efforts made since then have led to the successful applications of the TS-1/H₂O₂ catalytic system in innovative commercial processes for clean production of cyclohexanone oxime and propylene oxide.⁹

However, TS-1 suffers a major problem that its medium pores of 10-membered rings (MR) impose serious mass transfer limitations to substrates with relatively large molecular sizes. With the purpose to overcome the problems that TS-1 encounters in processing bulky substrates, researchers have developed many other titanosilicates with larger pores, either by hydrothermal

synthesis or by postsynthesis; for example, Ti-Beta,^{10,11} Ti-ZSM-12,¹² Ti-MOR,¹³ Ti-ITQ-7,¹⁴ Ti-MCM-68¹⁵ and Ti-MWW,^{16–18} all of which possess 12-MR channels or cages.

Among the above titanosilicates, Ti-MWW has attracted particular interest because not only is Ti-MWW itself a promising catalyst for epoxidation¹⁷ and ammoximation,^{19,20} but also the structural diversity of the MWW topology may convert Ti-MWW into titanosilicates with large porosity, and expand its abilities in catalytic applications. Structurally the same as the well-known MCM-22 aluminosilicate, the pore system of Ti-MWW is composed of 12-MR side cups and two independent interlayer and intralayer 10-MR channels, one of which contains the 12-MR supercages.^{21,22} Although it is characteristic of reversible structural interchange between 3-dimensional (3D) crystalline structure and the lamellar precursor,²³ once the 3D MWW structure is formed from the lamellar precursor through interlayer dehydration/condensation, the accessibility of the bulky molecules to the supercages is seriously restricted by the 10-MR pore window of the entrance. This limits the catalytic potential of the Ti active sites inside the supercages in the case of the oxidation of large molecules. Thus, the techniques of delamination, pillaring and interlayer expansion have been used to convert Ti-MWW into titanosilicates with open reaction spaces, such as the fully delaminated material Del-Ti-MWW,²⁴ the partially delaminated material Ti-MCM-56,²⁵ the interlayer pillared microporous-mesoporous hybrid material Ti-MCM-36²⁶ as well as the interlayer expanded material Ti-YNU-1.^{27,28} In comparison with 3D Ti-MWW, these titanosilicates generally show improved turnover number for the epoxidation of cyclic alkenes, as they not only preserve the basic structure unit of MWW zeolite but also possess more open pores or more accessible surfaces.

Nevertheless, the preparation procedures of Del-Ti-MWW and Ti-MCM-36 involve a troublesome sonication step difficult

^aShanghai Key Laboratory of Green Chemistry and Chemical Processes, Department of Chemistry, East China Normal University, North Zhongshan Rd. 3663, Shanghai, 200062, China. E-mail: pwwu@chem.ecnu.edu.cn; ymlu@chem.ecnu.edu.cn; Fax: +86-21 62232292

^bSchool of Urban Development and Environmental Engineering, Shanghai Second Polytechnic University, Jinhai Rd. 2360, Pudong, Shanghai, 201209, China

† This paper is part of a *Journal of Materials Chemistry* theme issue on Green Materials. Guest editors: James Clark and Duncan Macquarrie.

for scale-up synthesis, and also require the use of expensive reactants (cetyl trimethyl ammonium salts and tetrapropyl ammonium hydroxide). Ti-MCM-56 can be postsynthesized simply by controlling the acid treatment of the MWW precursor, but it lacks structural periodicity along the layer stacking direction, which leads to partial blocking of the intralayer channels.^{25,29} On the other hand, Ti-YNU-1 was obtained incidentally when refluxing with acid solution the Ti-MWW precursors postsynthesized through a reversible structural conversion route.²⁷ With an expanded interlayer spacing and well ordered stacking of MWW layers, Ti-YNU-1 proves to be a highly active, selective, and stable catalyst in the liquid-phase epoxidation of bulky alkenes. However, the formation of Ti-YNU-1 depends greatly on the Ti content of the precursors. It is obtained only when the Si/Ti ratio is higher than 70. It is expected that new methodology will be developed which can overcome this limitation and is possible to synthesize interlayer expanded materials independent of the Si/Ti ratio in Ti-MWW lamellar precursors. Thereafter, a structure elucidation by using the combination of HRTEM techniques and computational approach suggests that the structure of Ti-YNU-1 is probably constructed through interlayer pillaring with Si or Ti species.³⁰

This stimulated us to propose a feasible strategy to expand the interlayer space of layered zeolites in one step through alkoxy-silylating the corresponding lamellar precursors.³¹ Such a simple soft-chemical methodology expands efficiently the pore structure and avoids stepwise modifications such as interlayer expansion by ion-exchange with cationic surfactants, silylation, alcoholysis, and subsequent condensation usually required by layered silicas. With this unique interlayer silylation method, a series of interlayer expanded zeolites (IEZ) have been obtained successfully from the precursors of MWW, CDO, FER, MCM-47.^{31–34} Hence this method should open new possibilities for applying layered zeolites to petrochemical and fine-chemical industries. Since titanosilicates particularly with a large porosity are considered to weaken the adsorption restriction and diffusion limitation caused by the micropores of zeolites, and they are expected to be promising oxidation catalysts for processing large molecules, large-pore titanosilicates are urgently required in heterogeneous oxidation. By using the feasible technique previously developed to post-construct new zeolite structures,³¹ we have carried out the interlayer silylation of the lamellar precursors of Ti-MWW to prepare IEZ-Ti-MWW in this study. Its structure and porosity have been characterized, and its catalytic properties in the oxidation of alkenes have been investigated to show its potential application as a green heterogeneous catalyst.

Experimental

Synthesis of materials

Ti-MWW lamellar precursors with various Si/Ti ratios were hydrothermally synthesized using hexamethyleneimine (HMI) as a structure directing agent (SDA) from the gels with the molar compositions of 1.0 SiO₂ : (0–0.033) TiO₂ : 0.67 B₂O₃ : 1.4 HMI : 19 H₂O according to the previously reported procedures.³⁵ The precursors were alkoxy-silylated with different types of silylating agents such as diethoxydimethylsilane (Me₂Si(OEt)₂, DEDMS), triethoxymethylsilane (MeSi(OEt)₃), trimethylethoxysilane

(Me₃SiOEt) and tetraethyl orthosilicate (Si(OEt)₄, TEOS). Typically, 1 g of precursor was mixed with 20–50 g of an aqueous solution of HNO₃ (0–2 M) and the desired amount of silylating agent. The mixture was then refluxed at 373 K for 20 h to induce silylation. The amount of alkoxy-silane was varied in the range 0–0.3 g per gram of precursor. The silylated sample was filtered off and washed with deionized water repeatedly and dried at 393 K for 10 h. The samples were further calcined in air at 823 K for 10 h to remove any organic species. The resulting interlayer expanded zeolites are denoted as IEZ-Ti-MWW. As a control experiment, the precursors were also refluxed in 2 M HNO₃ solution and calcined at 823 K to obtain the usual titanosilicate with the 3D MWW, Ti-MWW.

Characterization methods

X-Ray powder diffraction (XRD) patterns were measured on a Bruker D8 ADVANCE diffractometer with Cu K α radiation. UV-visible diffuse reflectance spectra were recorded on a Shimadzu UV-2400PC spectrophotometer with BaSO₄ as a reference. Scanning electron microscopy (SEM) was performed on a Hitachi-4800 instrument after suspending the sample in ethanol. High resolution transmission electron microscopy (HRTEM) measurements were carried out with a 300 kV TEM (JEOL-3010, Cs 0.6 mm, resolution 1.7 Å). The ¹³C and ²⁹Si MAS NMR spectra were recorded on a Bruker DSX 300 multinuclear solid-state nuclear magnetic resonance spectrometer. FT-IR spectra were collected on a Nicolet Fourier transform infrared spectrometer (NEXUS 670) at room temperature using the KBr technique. Inductively coupled plasma (ICP) analysis was performed on a Thermo IRIS Intrepid II XSP atomic emission spectrometer. The elemental analyses for carbon and nitrogen contents were performed on an Elementar VarioEL III CHN elemental analyzer.

Catalytic reactions

The liquid-phase oxidation of cyclohexene with H₂O₂ was carried out to check the catalytic ability of titanosilicates for the oxidation of bulky molecules. The reactions were performed in a round-bottom flask (20 mL) equipped with a condenser. The temperature was controlled with a water bath. The reaction mixture containing 0.05 g of catalyst, 10 mL of acetonitrile as solvent, 10 mmol of cyclohexene or 1-hexene and 10 mmol H₂O₂ (31 wt% aqueous solution) as oxidant was stirred vigorously at 333 K for 2 h. The products were analyzed on a gas chromatograph (Shimadzu 14B, FID detector) equipped with a 30 m DB-1 capillary column using cyclohexanone as an internal standard. The amount of unconverted H₂O₂ was determined by the standard titration method using a 0.1 M Ce(SO₄)₂ solution.

Results and discussion

Interlayer silylation of Ti-MWW lamellar precursors

Ti-MWW lamellar precursor synthesized with a Si/Ti molar ratio of 20 was subjected to alkoxy-silylation in acidic media with the purpose to prepare highly crystalline materials with expanded pores. Diethoxydimethylsilane (DEDMS) with two ethoxy groups was first chosen to connect two up-and-down layers

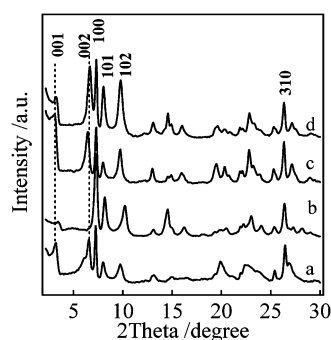


Fig. 1 XRD patterns of (a) as-synthesized Ti-MWW precursor (Si/Ti = 20), (b) sample a directly calcined (3D MWW), (c) sample a silylated with DEDMS, and (d) sample c further calcined (IEZ-Ti-MWW).

probably *via* condensation with the surface silanol groups. Meanwhile, the presence of two methyl groups would avoid the intermolecular condensation of the silane molecules themselves. Fig. 1 shows the XRD patterns of the lamellar precursor as well as the DEDMS-silylated samples before and after calcination. The pattern of the precursor was fully consistent with that of MWW-type lamellar precursor, which showed typical [001] and [002] diffractions in the 2θ region of $3\text{--}7^\circ$, characteristic of a layered structure along the c -direction (Fig. 1a). The layer structure is closely related to the interlayer occluded organic SDA molecules which serve as the pillaring species. A direct calcination of the lamellar precursor in air completely burned off the organic species, leading to the conventional 3D MWW structure.³⁵ Thus, it displayed an XRD pattern greatly different from that of the precursor (Fig. 1b). The [001] and [002] diffractions almost disappeared, while the diffractions assigned to the indexes of [h00] and [hk0], *i.e.* [100] and [310], remained practically unchanged. This implies that the structural change essentially takes place along the c -axis. The direct calcination caused the dehydroxylation and condensation between the layers, and then made the layer spacing decrease from 26.93 \AA for the precursor to 25.09 \AA for the 3D Ti-MWW (Table 1). As a result, the calcined sample had a narrower pore entrance between the layers than that of the original lamellar precursor.

When the precursor was silylated with DEDMS, the resulting sample still showed well resolved [001] and [002] diffractions in the 2θ region of $3\text{--}7^\circ$ with the [100] and [310] diffractions almost intact (Fig. 1c). Characteristic of a layered structure along the c -direction, the silylated sample seemed to be structurally similar to the MWW lamellar precursor obtained by direct hydrothermal synthesis. However, the silylated sample showed well resolved diffractions in the 2θ region of $10\text{--}25^\circ$ instead of

relatively broad ones, implying that it may possess ordered linkages between the MWW sheets rather than the hydrogen-bonded connection in the precursor. The structure of the silylated sample was thermally stable, as the calcination at 823 K did not cause obvious changes in its XRD pattern (Fig. 1d). The silylated sample had a layer spacing of 27.58 \AA (Table 1), which was slightly larger than that of the lamellar precursor. As the unit cell parameters along the a and b axes were almost same for the precursor, 3D MWW and the silylated sample, the structural change is considered to occur mainly along the direction of layer stacking. In comparison with 3D MWW, the silylation expanded the pore windows at least by *ca.* 2.5 \AA between the layers, leading to interlayer expanded zeolite of MWW sheet-containing titanosilicate, IEZ-Ti-MWW. The N_2 adsorption indicated that IEZ-Ti-MWW with an open porosity had a higher specific surface area than 3D Ti-MWW (Table 1).

Using the lamellar precursor synthesized at a Si/Ti ratio of 20 as a parent sample, we investigated in detail the effect of silylation conditions on the structural transformation to IEZ-Ti-MWW. The formation of ordered structure of interlayer expansion depended on the used amount of silylating agent. As shown in Fig. 2, the 3D Ti-MWW sample was obtained when the lamellar precursor was refluxed in 2 M HNO_3 and further calcined at 823 K (Fig. 2b). The diffraction due to the [002] plane shifted to higher angle and was almost invisible as it was hidden by the [100] diffraction. The silylation treatments of the precursor with different amounts of DEDMS all led to the IEZ-Ti-MWW structure showing [002] diffraction, the intensity of which increased gradually with increasing amount of DEDMS. When the amount of DEDMS used was 0.025 g per gram of the

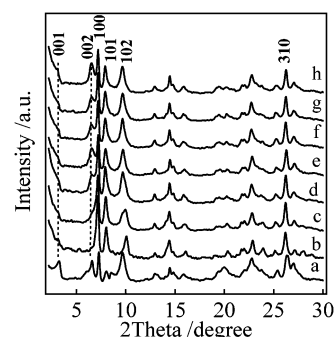


Fig. 2 XRD patterns of (a) as-synthesized Ti-MWW precursor (Si/Ti = 20), (b) 3D Ti-MWW, and IEZ-Ti-MWW prepared by silylation with (c) 0.025 g , (d) 0.05 g , (e) 0.07 g , (f) 0.1 g , (g) 0.15 g , (h) 0.3 g of DEDMS per gram of the precursor in 2 M HNO_3 after further calcination in air at 823 K for 10 h .

Table 1 The unit cell parameters and specific surface areas of Ti-MWW lamellar precursor, 3D Ti-MWW and IEZ-Ti-MWW

Sample	Unit cell parameters (\AA) ^a			SSA ($\text{m}^2\text{ g}^{-1}$) ^b
	<i>a</i>	<i>b</i>	<i>c</i>	
Ti-MWW lamellar precursor	14.15	14.15	26.93	ND ^c
3D Ti-MWW	14.19	14.19	25.09	530
IEZ-Ti-MWW	14.10	14.10	27.58	560

^a Given by XRD. ^b SSA, specific surface area measured by N_2 adsorption at 77 K . ^c Not determined.

precursor, the intensity of the [002] diffraction was very weak, indicating that the amount of DEDMS was not enough to connect the up-and-down layers. The more DEDMS used, the more intense [002] diffraction was observed as a result of the gradually expanded layer structure along the *c*-direction (Fig. 2c–h). This indicates that it is possible to control the phase purity and crystallinity of IEZ-Ti-MWW by adjusting the extent of silylation. When the amount of DEDMS was more than 0.15 g per gram of the precursor, the intensity of the [002] diffraction displayed no obvious distinction, suggesting that a saturated incorporation of silane groups could be realized at an optimal weight ratio of silane to precursor of 0.15 g g⁻¹.

IR spectroscopy was employed to monitor the silylation processes. Fig. 3 shows the IR spectra of the samples prepared by silylating the lamellar precursor with different amounts of DEDMS in 2 M HNO₃ solution but without calcination. The acid treated Ti-MWW precursor in the absence of DEDMS showed the bands at 2926 and 2850 cm⁻¹ (Fig. 3a), which are due to the stretching vibration of CH₂ groups originating from the HMI molecules incorporated in the pores during precursor crystallization. The HMI molecules are reported to occupy both the interlayer space and the intralayer 10-MR channels.³⁶ The cyclic HMI molecules with a relatively large dimension were not extracted completely by the acid treatment, as the organic molecules were confined firmly in the intralayer sinusoidal channels in addition to the interlayer pores. Thus, the 2926 and

2850 cm⁻¹ bands were still observed after the silylation although they decreased slightly in intensity. The silylation, however, resulted in two bands at 2970 and 850 cm⁻¹ (Fig. 3b–g). These bands were absent for the sample obtained by the acid treatment without DEDMS, and are assigned to the CH₃ asymmetric stretching vibration and the rocking of CH₃ groups attached to Si, respectively.^{37,38} This confirmed the incorporation of the (CH₃)₂Si moiety into the material. The intensity of the 2970 and 850 cm⁻¹ bands increased with increasing amount of DEDMS, and was almost leveled off when the weight ratio of DEDMS to precursor was over 0.15 g g⁻¹.

The amount of DEDMS actually incorporated was analyzed by elemental analysis (Table 2). The precursor had a C/N molar ratio of 5.88, which was very close to that of HMI, suggesting the organic species existed inside the zeolite channels in the form of HMI molecules. In comparison with the precursor, the silylation in acid solution made the contents of both carbon and nitrogen decrease as a result of removal of HMI species located mainly in the interlayer space (Table 2, Nos. 2–5). Nevertheless, the carbon content of the silylated samples increased slightly with increasing amount of DEDMS, resulting in gradually increased C/N ratio (Table 2, fifth column). This can be taken as evidence for the incorporation of the silylating agent. The amount of carbon actually gained by silylation was obtained by extracting from the total carbon content sample with the remaining HMI species which was determined on the basis of the nitrogen content (Table 2, sixth column). The number of DEDMS molecules incorporated per unit cell was then calculated according to the incorporated carbon and the chemical composition of samples (Table 2, seventh column). According to the structure of the MWW topology,²¹ every unit cell has two pillaring sites between the layers. When the weight ratio of DEDMS to precursor was over 0.15 g g⁻¹, the silane molecules incorporated per unit cell were enough to consume the interlayer silanols to induce structural expansion, and even to silylate other sites such as surface silanols and/or internal silanols on defect sites.

Fig. 4 shows the XRD patterns of IEZ-Ti-MWW prepared by the silylation with 0.15 g DEDMS per gram of the precursor in different concentrations of HNO₃ to investigate the influence of acid concentration on the formation of IEZ-Ti-MWW. When the amount of DEDMS was fixed at 0.15 g per gram of Ti-MWW lamellar precursor, IEZ-Ti-MWW was obtained in a wide range of acid concentration. The acid concentration did not show obvious influence on the intensity of the [002] diffraction,

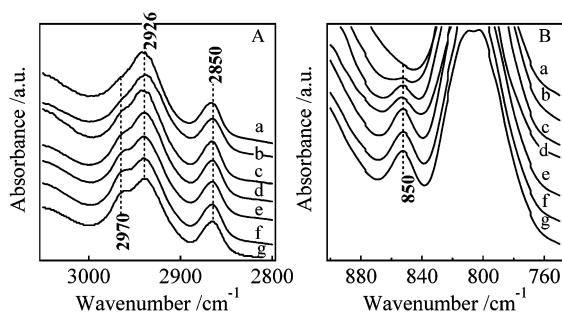


Fig. 3 FT-IR spectra of (a) acid treated Ti-MWW with 2M HNO₃, and IEZ-Ti-MWW prepared by silylation with (b) 0.025 g, (c) 0.05 g, (d) 0.07 g, (e) 0.1 g, (f) 0.15 g, (g) 0.3 g of DEDMS per gram of the precursor in 2 M HNO₃ without calcination. The silylation resulted in bands at 2970 and 850 cm⁻¹ assigned to the asymmetric vibration CH₃ groups and the rocking vibration of Si–CH₃, respectively.

Table 2 The results of chemical analyses after the silylation of Ti-MWW lamellar precursor with different amounts of DEDMS

No.	DEDMS ^a (g g ⁻¹)	Amount (wt%)		C/N ^b	C incorporated ^c (wt%)	DEDMS incorporated ^d (molecule per unit cell)
		C	N			
1	0	10.23	2.03	5.88	0	0
2	0.05	8.70	1.48	6.86	1.09	1.9
3	0.10	8.95	1.46	7.15	1.44	2.6
4	0.15	9.13	1.45	7.38	1.67	3.0
5	0.30	9.26	1.46	7.40	1.75	3.1

^a The amount of DEDMS used per gram of lamellar precursor in the silylation. ^b Molar ratio. The precursor had a C/N molar ratio of 5.88, similar to that of SDA of HMI. ^c Calculated by deducting the C amount of HMI from the total amount of C according to the equation: C – (N/14) × 6 × 12.

^d Every two incorporated C atoms correspond to one DEDMS molecule.

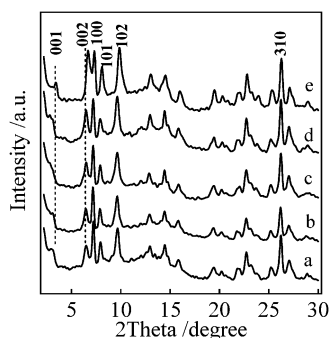


Fig. 4 XRD patterns of IEZ-Ti-MWW prepared by the silylation with 0.15g DEDMS per gram of the precursor in different concentration of HNO_3 (a) 0.1 M, (b) 0.3 M, (c) 0.5 M, (d) 1 M, (e) 2 M and further calcined in air at 823 K for 10 h.

indicating the interlayer expansion can be realized effectively under mild conditions in 0.1 M HNO_3 solution.

Fig. 5 shows the XRD patterns of the Ti-MWW samples with various Si/Ti molar ratios prepared without or with the silylation treatment. The 3D Ti-MWW samples were obtained readily from the corresponding lamellar precursors by calcination at 823 K in air, which made the layer-related [001] and [002] diffractions disappear completely (Fig. 5A). However, when the precursors were silylated with DEDMS at a silane to precursor weight ratio of 0.15 g g^{-1} in 1 M HNO_3 solution, IEZ-Ti-MWW materials with different Si/Ti molar ratios were obtained. They were all featured by developing the [001] and [002] diffractions (Fig. 5B), and then by expanded pore windows between the layers. It is worth mentioning that the formation of the IEZ structure by the present silylation method was independent of the Si/Ti molar ratio in the precursors which could be hydrothermally synthesized. This would overcome the limitation encountered in the preparation of Ti-YNU-1, in which the expanded pore structure can only be constructed for the postsynthesized lamellar precursors with $\text{Si/Ti} > 70$.^{27,28}

In addition to DEDMS, other monomeric silylating agents such as tetraethoxysilane (TEOS), triethoxymethylsilane and trimethylethoxysilane were also employed to induce the structure expansion. The molar amount of the different types of silylating agent used was comparable to 0.15 g of DEDMS per gram of precursor. The intensity of the [002] diffraction had no obvious distinction among the samples prepared using different silylating

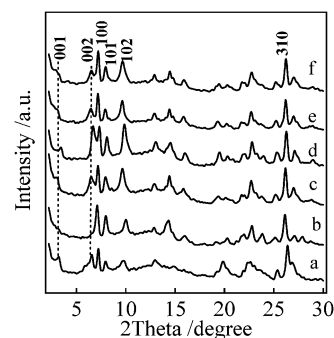


Fig. 6 XRD patterns of (a) lamellar precursor, (b) 3D Ti-MWW, and IEZ-Ti-MWW prepared by the silylation with (c) $\text{Si}(\text{OEt})_4$, (d) $\text{MeSi}(\text{OEt})_3$, (e) DEDMS, (f) Me_3SiOEt and further calcined in air at 823 K for 10 h.

agents (Fig. 6), indicating these silanes are all applicable to induce the interlayer expansion. In the process of silylation, the molecules of monomeric silanes react with the silanol groups on the layer surface to realize incorporation of silane groups and formation of Si–O–Si linkages. The subsequent calcination burns off the methyl groups coordinated to the Si atoms as well as the SDA species occluded in the pores, leading to a new pore structure which is composed of the $\text{Si}(\text{OH})_2$ pillar together with the original framework T atoms.³¹ According to this possible mechanism of interlayer silylation and pore expansion, it is anticipated that the above four monomeric silylating agents can serve as pore expansion pillars. Nevertheless, TEOS with four ethoxy groups was inclined to impose a serious intermolecular condensation after hydrolysis in acid solution, which led to the deposition of amorphous silica on the zeolite crystals. This may influence the catalytic activity of the corresponding IEZ-Ti-MWW, to be shown later. Although trimethylethoxysilane has only one ethoxy group available for the silylation with silanol, it is presumed that once the Me_3Si – group was attached to a MWW sheet through Si–O–Si bonding, the connection to the other sheet also *via* Si–O–Si bonding could be achieved during the process of CH_3 group removal by calcination.

Characterization of IEZ-Ti-MWW

The UV-visible spectra of the as-synthesized Ti-MWW precursor, 3D Ti-MWW and IEZ-Ti-MWW are shown in Fig. 7.

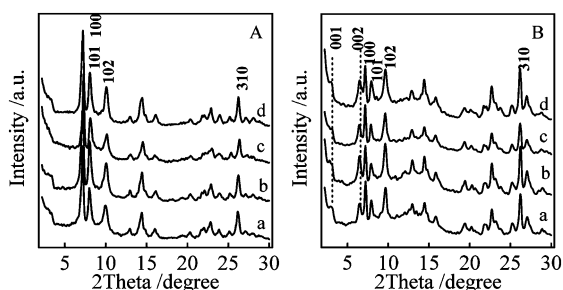


Fig. 5 XRD patterns of (A) 3D Ti-MWW and (B) IEZ-Ti-MWW produced from the same lamellar precursors hydrothermally synthesized at Si/Ti molar ratios of (a) 30, (b) 50, (c) 70, (d) 100.

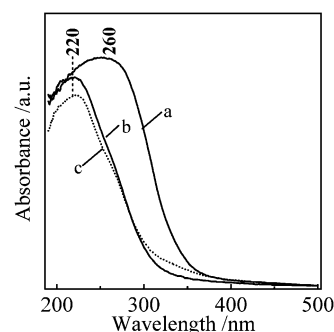


Fig. 7 UV-visible spectra of (a) as-synthesized Ti-MWW ($\text{Si/Ti} = 20$), (b) 3D Ti-MWW, and (c) IEZ-Ti-MWW.

The precursor synthesized at a Si/Ti molar ratio of 20 exhibited a main band at 260 nm together with a weak shoulder around 220 nm (Fig. 7a). The 220 nm band, resulting from the charge transfer from O^{2-} to Ti^{4+} , has been widely found for Ti-substituted zeolites and is characteristic of tetrahedrally coordinated Ti species highly dispersed in the framework.^{4,5} The 260 nm band has been attributed to octahedral Ti species. The occurrence of the 260 nm band for the present samples is presumed to be closely related to the layered structure of the MWW precursor irrespective of the Si/Ti ratio in synthetic gels.³⁵ The layer surface is favorable for the incorporation of octahedral Ti therein. These octahedral Ti species are usually removed selectively by refluxing the precursor in acid solution before calcination, resulting in 3D Ti-MWW which showed only the 220 nm band assigned to tetrahedral Ti (Fig. 7b). The acid treatment at 373 K for 20 h in the presence of silylating agent also extracted the extraframework species effectively (Fig. 7c), suggesting the presence of DEDMS had no negative effect on the removal of the octahedral Ti species. This phenomenon was clearly observed for the IEZ-Ti-MWW samples prepared with different amounts of silylating agent, as they showed only the narrow 220 nm band in the UV-visible spectra (Fig. 8).

The crystals of Ti-MWW precursor showed the morphology of platelets (*ca.* $1 \times 1 \times 0.1 \mu\text{m}$) which generally formed aggregates of 10–15 μm size (not shown). 3D Ti-MWW obtained by the acid treatment of the precursor showed the same morphology (Fig. 9a). Upon acid refluxing in the presence of silylating agent, that is, after forming the interlayer expanded crystalline structure, no change in morphology was observed (Fig. 9b). These results confirmed that the morphologies were preserved after the chemical modification. The structural expansion is therefore

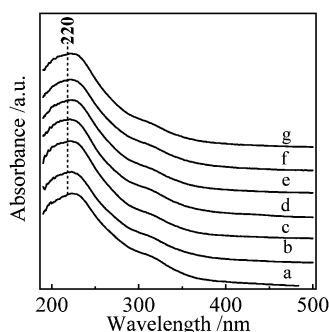


Fig. 8 UV-Visible spectra of (a) 3D Ti-MWW, and IEZ-Ti-MWW prepared by silylation with (b) 0.025 g, (c) 0.05 g, (d) 0.07 g, (e) 0.1 g, (f) 0.15 g, (g) 0.3 g of DEDMS per gram of the precursor (Si/Ti = 20) in 2 M HNO_3 and further calcined in air at 823 K for 10 h.

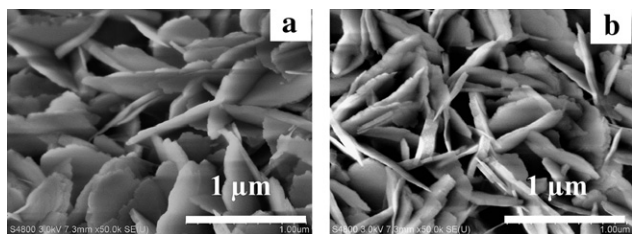


Fig. 9 SEM images of (a) Ti-MWW, (b) IEZ-Ti-MWW.

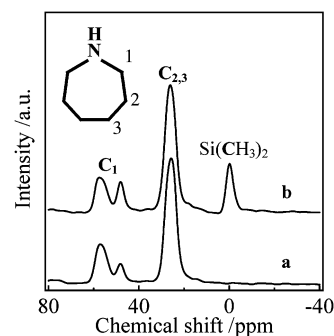


Fig. 10 ^{13}C MAS NMR spectra of (a) Ti-MWW lamellar precursors, and (b) after silylation with DEDMS in 2 M HNO_3 without calcination. The silylation resulted in a signal at -2.0 ppm assigned to carbon species in $\text{Si}(\text{CH}_3)_2$ groups.

assumed to take place at a sub-nanometer level but not a micrometer scale of the crystals.

The incorporation of $(\text{CH}_3)_2\text{Si}$ groups into the lamellar precursor by silylation has been further investigated by ^{13}C and ^{29}Si MAS NMR techniques. The ^{13}C MAS NMR spectra of Ti-MWW lamellar precursor and the silylated sample without calcination both showed resonances at 48.5, 57 and 26.5 ppm (Fig. 10). The former two resonances, assigned to the carbon species at C_1 position of HMI, are presumably associated with the residence of HMI in two distinct void spaces, that is, interlayer channels and intralayer channels.³⁶ The latter one is attributed to the overlapped signals of the carbon species at the C_2 and C_3 positions of HMI. What is more attractive is that the silylation developed a new resonance at -2.0 ppm in the ^{13}C MAS NMR spectrum (Fig. 10b), which is due to the configuration of $(\text{CH}_3)_2\text{Si}$ groups.³⁷

The ^{29}Si MAS NMR spectra provided structural information complementary to that given by the above diffraction techniques. The Ti-MWW lamellar precursor and the silylated sample without calcination showed the main resonances at -110 and -120 ppm (Fig. 11), which are attributed to the silicon atoms coordinated with four silicon atoms (Q^4). In addition, the precursor showed an obvious resonance at -103 ppm due to the

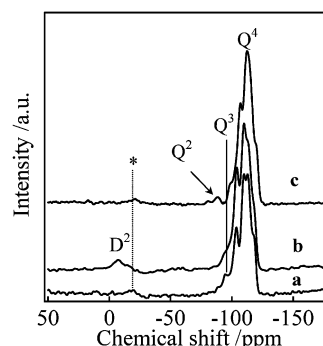


Fig. 11 ^{29}Si MAS NMR spectra of (a) Ti-MWW lamellar precursor, (b) after silylation with DEDMS in 2 M HNO_3 without calcination, and (c) after further calcination at 823 K. The silylation consumed a portion of the silanol groups (Q^3) and developed at -12 ppm a signal assigned to $=\text{Si}(\text{CH}_3)_2$ groups (D^2) instead, which were converted to $=\text{Si}(\text{OH})_2$ groups (Q^2) around -90 ppm after calcination.

Q^3 site, $Si(OH)(OSi)_3$ or $Si(OH)(OTi)(OSi)_2$. Compared with the precursor, the silylated sample showed a much less intense -103 ppm resonance, while the samples exhibited a new resonance at -12 ppm (Fig. 11b). This signal is attributed to the silicon atom from $Si(CH_3)_2(OSi)_2$ groups (D^2).³⁹ The results further confirmed that the silylation occurred through the reaction of silane groups with the silanols on the layer surface to form pillaring silicon species between the layers. When the silylated sample was further calcined at 823 K, the organic species including the methyl groups and remaining HMI were burned off completely. The D^2 signal disappeared, whereas the signal corresponding to the Q^2 groups, $Si(OH)_2(OSi)_2$, was observed at *ca.* -90 ppm. This suggests that the incorporated silane groups lost the methyl moieties, but the Si species cross-linked to the MWW sheets remained in the interlayer spaces to pillar the expanded pore structure.

The changes in pore structure as a result of silylation were investigated by HRTEM measurement. The TEM image taken of the platelet crystal surface, that is along the $[001]$ incidence, is shown in Fig. 12a together with the corresponding Fourier diffractogram (FD). IEZ-Ti-MWW had ordered arrays of 12-MR side cups or side pockets in this projection, which is almost the same as that of the normal 3D MWW structure reported previously, and reveals the characteristic hexagonal framework topology of MWW type materials.^{27,30} The image did not show any aperiodically or periodically repeating defects. It is thus apparent that the silylation did not alter the structure within the MWW sheets. The TEM image and FD taken perpendicular to the side of the platelet, that is along the $[100]$ incidence, indicated that IEZ-Ti-MWW also showed a well ordered pore structure along the stacking direction of MWW sheets (Fig. 12b). It is concluded that analogous to the 3D MWW topology, IEZ-Ti-MWW also has a 3D-connected framework structure composed of MWW sheets. This should be a result of uniform silylation achieved throughout the crystals. The average layer spacing of IEZ-Ti-MWW was 27.4 Å, while that of 3D Ti-MWW was 25 Å as reported previously.³⁰ In agreement with the data given by XRD (Table 1), the silylation caused an expansion in the c direction of *ca.* 2.4 Å. This would contribute mainly to the enlargement of pore windows between the layers in IEZ-Ti-MWW. Although the real structure of IEZ-MWW is still waiting for structural resolution by synchrotron X-ray diffraction, a 12-MR pore window is suggested to be constructed by inserting two pillaring Si species between the layers, instead of 10-MR pores of 3D MWW.

On the basis of the aforementioned XRD, IR, NMR and HRTEM investigations, the procedures for interlayer silylation, pore expansion and formation of regular large pores between the layers are graphically described in Scheme 1 using DEDMS as a representative silylating agent. In acid solution, the SDA molecules were extracted from the interlayer space, making the silane molecules accessible to the silanol groups on the layer surface to induce silylation. The formation of Si–O–Si bonds with up-and-down layers resulted in the incorporation of the silane groups, while the interlayer structure expanded. Finally, a large-pore titanosilicate, IEZ-Ti-MWW, was obtained.

XRD and HRTEM investigations verified consistently that the structure of IEZ-Ti-MWW was very similar to that of previously reported Ti-YNU-1.³⁰ However, the present silylation method is

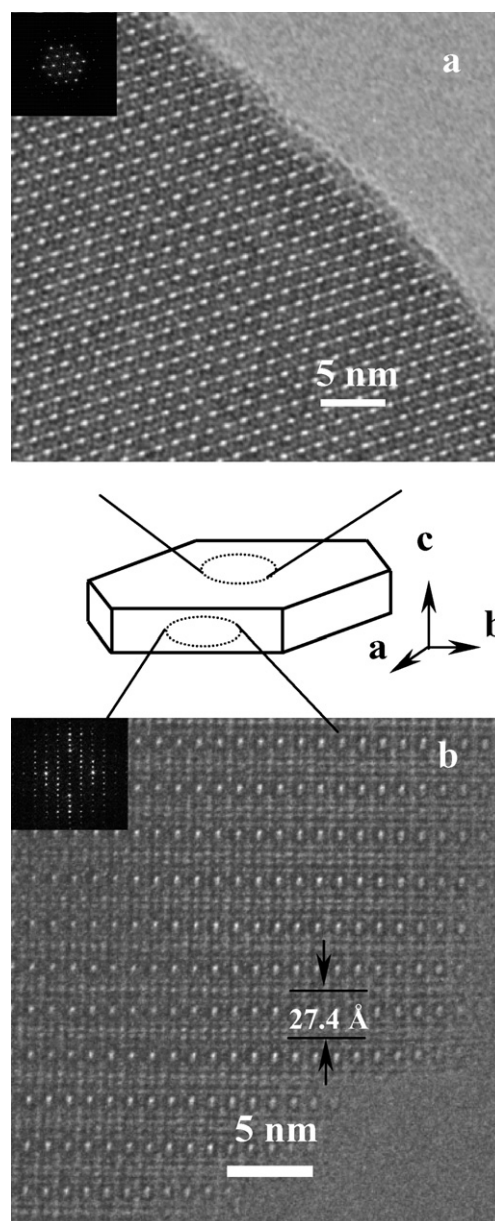
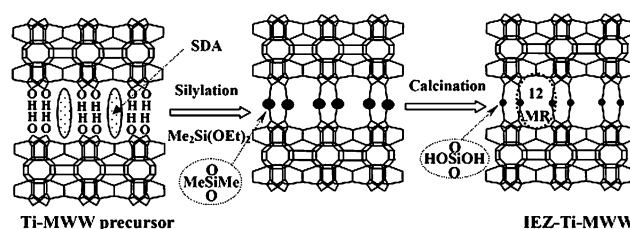


Fig. 12 TEM images of IEZ-Ti-MWW taken along (a) $[001]$ incidence and (b) $[100]$ incidence. FDs are also inset in the images.



Scheme 1

independent of the Ti content of precursors, and proves to be more feasible and useful for the preparation of large-pore titanosilicates.

Catalytic properties of IEZ-Ti-MWW

Ti-MWW has been reported to be a promising catalyst for the epoxidation of various linear alkenes with H_2O_2 as an oxidant.^{17,40,41} The IEZ materials, having larger pores than the 3D MWW structure, are expected to show higher catalytic activities especially for bulky molecules. We thus investigated the catalytic properties of IEZ-Ti-MWW in the epoxidation of 1-hexene and cyclohexene.

Table 3 compares the results of liquid-phase epoxidation of 1-hexene and cyclohexene with H_2O_2 between 3D Ti-MWW and IEZ-Ti-MWW samples prepared with different amounts of silylating agent. The molecules of linear 1-hexene are small enough to enter into both the interlayer and intralayer 10-MR channels of the 3D MWW structure, and reach readily the active Ti sites without mass transfer limitation. Thus, 3D Ti-MWW and IEZ-Ti-MWW show no obvious differences in the oxidation of 1-hexene. In contrast, the cyclohexene molecules with a larger kinetic diameter hardly penetrate the distorted intralayer 10-MR channels. Actually, the Ti sites in the supercages of 3D MWW are potential active sites for the oxidation of bulky molecules, but the entrance of bulky molecules into the supercages is seriously restricted by the 10-MR windows. Thus, for 3D Ti-MWW, only the Ti sites on the external surface and within the side pockets are considered to act as active sites for the oxidation of cyclohexene. Since the 2D intralayer sinusoidal 10-MR channels are not connected to the supercages, the interlayer space expansion is the most effective way to make the Ti sites in the supercages available for oxidizing bulky substrate molecules. As described above, a saturated incorporation of silane groups was realized at a silane to precursor weight ratio of 0.15 g g⁻¹. Consequently, the accessibility of the Ti sites to cyclohexene molecules was the highest for the IEZ-Ti-MWW prepared under that condition. This sample exhibits a turnover number (TON) about 7 times that of 3D Ti-MWW. But once the addition amount of DEDMS exceeded 0.15 g g⁻¹, the activity declined probably due to pore blocking by the condensation of the excess silanes. Therefore, it is necessary to use an optimal amount of DEDMS to achieve active catalysts for bulky molecules.

To further ensure the activity improvement by alkoxysilylation, 3D Ti-MWW and IEZ-Ti-MWW with different Ti contents were checked in the epoxidation of cyclohexene with H_2O_2 (Fig. 13). As

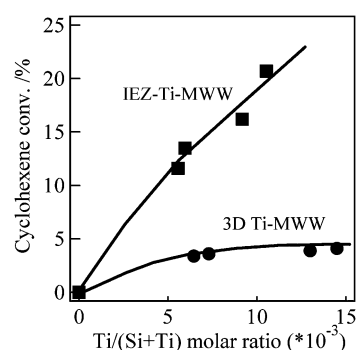


Fig. 13 Comparison of the catalytic activity between 3D Ti-MWW and IEZ-Ti-MWW with different Si/Ti mole ratios in the epoxidation of cyclohexene. Reaction conditions: cat., 0.05 g; cyclohexene, 10 mmol; H_2O_2 , 10 mmol; MeCN, 10 mL; temp., 333 K; time, 2 h.

expected the cyclohexene conversion increased with increasing amount of Ti active sites for both 3D Ti-MWW and IEZ-Ti-MWW. However, the increase was very limited in the case of 3D Ti-MWW, as only the Ti species are usable for this reaction. IEZ-Ti-MWW, with expanded interlayer pores and the Ti species inside the supercages accessible to the cyclohexene molecules, showed much higher conversion than 3D Ti-MWW. The distinction became more obvious at a higher Ti content.

Table 4 lists the catalytic properties obtained on the IEZ-Ti-MWW catalysts which were prepared using different types of silylating agents. TEOS was inclined to induce serious intermolecular condensation, which led to the deposition of amorphous silica on the zeolite crystals. The IEZ-Ti-MWW prepared with TEOS thus showed a lower activity in comparison with the others. The methyl groups contained in triethoxymethylsilane, trimethylethoxysilane and DEDMS effectively restrained the condensation of silane molecules, leading to IEZ-Ti-MWW showing much higher activity than that prepared with TEOS. The IEZ-Ti-MWW catalysts also had an advantage in product selectivity. They showed higher epoxide selectivities (43.3–57.1%) than conventional 3D Ti-MWW (32.5%).

As a result, the expanded structure enhanced greatly the catalytic activity of Ti-MWW in the epoxidation of alkenes with bulky molecular dimensions. This implies that the post-treatment through alkoxysilylating the Ti-MWW lamellar precursor is an

Table 3 The catalytic activity obtained on 3D Ti-MWW and IEZ-Ti-MWW synthesized with different amounts of DEDMS in the epoxidation of 1-hexene and cyclohexene^a

Catalyst		Cyclohexene oxidation						1-Hexene oxidation					
DEDMS (g g ⁻¹)	Si/Ti	Conv. (mol%)	TON ^b	Product sel. (mol%)		H ₂ O ₂ (mol%)		Conv. (mol%)	Product sel. (mol%)		H ₂ O ₂ (mol%)		
				oxide	others ^c	conv.	sel.		oxide	others ^c	conv.	sel.	
0	68	4.1	33	41	59	4.6	89	13.1	92.7	7.3	19.6	66.7	
0.025	95	9.2	105	39	61	11.2	79	10.2	95.6	4.4	15.2	63.0	
0.05	86	14.4	149	59	41	20.6	72	13.9	96.8	3.2	20.1	63.8	
0.07	94	15.3	172	41	59	17.0	92	9.1	93.0	7.0	12.0	75.8	
0.1	82	15.8	159	58	42	20.1	75	12.6	95.6	4.4	15.8	79.7	
0.15	94	20.7	233	57	43	19.9	98	12.1	95.0	5.0	17.6	68.8	
0.3	105	14.2	178	36	64	16.0	89	9.8	95.6	4.4	15.1	64.9	

^a Reaction conditions: cat., 0.05 g; alkenes, 10 mmol; H_2O_2 , 10 mmol; MeCN, 10 mL; temp., 333 K; time, 2 h. ^b TON in mol (mol Ti)⁻¹ which was calculated by dividing the amount of alkene converted with the used Ti amount. ^c 2-Cyclohexene-1-ol, 2-cyclohexene-1-one, glycols.

Table 4 The catalytic properties shown by 3D Ti-MWW and IEZ-Ti-MWW prepared with different silylating agents in the oxidation of cyclohexene^a

Silylating agent	Cyclohexene oxidation				
	Conv.(mol%)	Product sel. (mol%)		H ₂ O ₂ (mol%)	
		oxide	others ^b	conv.	sel.
None	4.1	32.5	67.5	5.6	69.6
TEOS	8.8	43.3	56.7	9.4	92.9
Triethoxymethylsilane	19.2	53.5	46.5	20.4	90.3
Trimethylethoxysilane	19.8	54.6	45.4	21.0	94.3
DEDMS	20.7	57.1	42.9	19.9	98.3

^a Reaction conditions: cat., 0.05 g; cyclohexene, 10 mmol; H₂O₂, 10 mmol; MeCN, 10 mL; temp., 333 K; time, 2 h. ^b 2-Cyclohexene-1-ol, 2-cyclohexene-1-one, glycols.

effective way to obtain crystalline zeolites with enlarged pores useful for fine chemical synthesis.

Conclusions

The alkoxysilylating treatment of Ti-MWW lamellar precursor leads to new crystalline titanosilicates having an interlayer expanded structure in comparison with the conventional 3D Ti-MWW. The expanded structure is formed as a result of the incorporated Si species serving as pillars. The silylation process is independent of Ti content in directly synthesized Ti-MWW precursors, leading to IEZ-Ti-MWW catalysts with a wide range of Ti content. Compared with 3D Ti-MWW, IEZ-Ti-MWW contains much more open interlayer spaces, showing a significantly improved catalytic activity in the liquid-phase epoxidation of alkenes with large molecular dimensions. IEZ-Ti-MWW is expected to open up green oxidation processes for synthesizing large oxygenated fine chemicals. This study may offer a new route for designing and preparing large-pore titanosilicate catalysts.

Acknowledgements

We gratefully acknowledge the NSFC of China (20673038, 20873043), Science and Technology Commission of Shanghai Municipality (08JC1408700, 09XD1401500, 07QA14017, 08QA1402700), 973 Program (2006CB202508), 863 Program (2007AA03Z34), and Shanghai Leading Academic Discipline Project (B409). Y.W. thanks the PhD Program Scholarship Fund of ECNU 2008. We thank Dr Juanfang Ruan for measuring the HRTEM images and helpful discussion.

References

- 1 *Peroxide-Chemie: Langkettige Alpha-Epoxide*, Höllriegelskreuth, Chapters 1–4, pp. 1–29, 1981.
- 2 T. Taramasso, G. Perego and B. Notari, *US Pat.* 1983, 441050.
- 3 M. G. Clerici, G. Bellussi and U. Romano, *J. Catal.*, 1991, **129**, 159.
- 4 G. Bellussi and M. S. Rigutto, *Stud. Surf. Sci. Catal.*, 2001, **137**, 911.
- 5 P. Ratnasamy, D. Srinivas and H. Knözinger, *Adv. Catal.*, 2004, **48**, 1.
- 6 B. Notari, *Adv. Catal.*, 1996, **41**, 253.
- 7 M. G. Clerici and P. Ingallina, *J. Catal.*, 1993, **140**, 71.
- 8 A. Corma, M. A. Camblor, P. Esteve, A. Martínez and J. Pérez-Pariente, *J. Catal.*, 1994, **145**, 151.
- 9 H. Ichihashi and H. Sato, *Appl. Catal., A*, 2001, **221**, 359.
- 10 A. Corma, P. Esteve, A. Martínez and S. Valencia, *J. Catal.*, 1995, **152**, 18.
- 11 T. Tatsumi and N. Jappari, *J. Phys. Chem.*, 1998, **102**, 7126.
- 12 A. Tuel, *Zeolites*, 1995, **15**, 236.
- 13 (a) P. Wu, T. Komatsu and T. Yashima, *J. Phys. Chem.*, 1996, **100**, 10316; (b) P. Wu, T. Komatsu and T. Yashima, *J. Phys. Chem. B*, 1998, **102**, 9297.
- 14 M. Diaz-Cabanas, L. A. Villaescusa and M. A. Camblor, *Chem. Commun.*, 2000, 761.
- 15 Y. Kubota, Y. Koyama, T. Yamada, S. Inagaki and T. Tatsumi, *Chem. Commun.*, 2008, 6224.
- 16 P. Wu, T. Tatsumi, T. Komatsu and T. Yashima, *Chem. Lett.*, 2000, 774.
- 17 P. Wu, T. Tatsumi, T. Komatsu and T. Yashima, *J. Catal.*, 2001, **202**, 245.
- 18 P. Wu and T. Tatsumi, *Chem. Commun.*, 2001, 897.
- 19 F. Song, Y. Liu, H. Wu, M. He, P. Wu and T. Tatsumi, *J. Catal.*, 2006, **237**, 359.
- 20 F. Song, Y. Liu, L. Wang, H. Zhang, M. He and P. Wu, *Appl. Catal., A*, 2007, **327**, 22.
- 21 M. E. Leonowicz, J. A. Lawton and S. L. Lawton, *Science*, 1994, **264**, 1910.
- 22 S. L. Lawton, M. E. Leonowicz and P. D. Partridge, *Microporous Mesoporous Mater.*, 1998, **23**, 109.
- 23 L. Wang, Y. Liu, W. Xie, H. Wu, X. Li, M. He and P. Wu, *J. Phys. Chem. C*, 2008, **112**, 6132.
- 24 P. Wu, D. Nuntasri, J. Ruan, Y. Liu, M. He, W. Fan, O. Terasaki and T. Tatsumi, *J. Phys. Chem. B*, 2004, **108**, 9126.
- 25 L. Wang, Y. Wang, Y. Liu, L. Chen, S. Cheng, G. Gao, M. He and P. Wu, *Microporous Mesoporous Mater.*, 2008, **113**, 435.
- 26 S. Kim, H. Ban and W. Ahn, *Catal. Lett.*, 2007, **113**, 160.
- 27 W. Fan, P. Wu, S. Namba and T. Tatsumi, *Angew. Chem., Int. Ed.*, 2004, **43**, 236.
- 28 W. Fan, P. Wu, S. Namba and T. Tatsumi, *J. Catal.*, 2006, **243**, 183.
- 29 G. Juttu and R. Lobo, *Microporous Mesoporous Mater.*, 2000, **40**, 9.
- 30 J. Ruan, P. Wu, B. Slater and O. Terasaki, *Angew. Chem., Int. Ed.*, 2005, **44**, 6719.
- 31 P. Wu, J. Ruan, L. Wang, L. Wu, Y. Wang, Y. Liu, W. Fan, M. He, O. Terasaki and T. Tatsumi, *J. Am. Chem. Soc.*, 2008, **130**, 8178.
- 32 S. Inagaki and T. Tatsumi, *Chem. Commun.*, 2009, 2583.
- 33 S. Inagaki, T. Yokoi, Y. Kubota and T. Tatsumi, *Chem. Commun.*, 2007, 5188.
- 34 J. Ruan, P. Wu, B. Slater, Z. Zhao, L. Wu and O. Terasaki, *Chem. Mater.*, 2009, **21**, 2904.
- 35 P. Wu, T. Tatsumi, T. Komatsu and T. Yashima, *J. Phys. Chem. B*, 2001, **105**, 2897.
- 36 S. L. Lawton, A. S. Fung, G. J. Kennedy, L. B. Alemany, C. D. Chang, G. H. Hatzikos, D. N. Lissy, M. K. Rubin, H.-K. C. Timken, S. Steuernagel and D. E. Woessner, *J. Phys. Chem.*, 1996, **100**, 3788.
- 37 J. Joo, T. Hyeon and J. Hyeon-Lee, *Chem. Commun.*, 2000, 1487.
- 38 K. Yamamoto, Y. Nohara, Y. Domon, Y. Takahashi, Y. Sakata, J. Plévert and T. Tatsumi, *Chem. Mater.*, 2005, **17**, 3913.
- 39 G. Engelhardt and D. Michel, *High-Resolution Solid-State NMR of Silicates and Zeolites*; John Wiley & Sons Ltd.: New York, 1987.
- 40 P. Wu and T. Tatsumi, *J. Catal.*, 2003, **214**, 317.
- 41 L. Wang, Y. Liu, W. Xie, H. Zhang, H. Wu, Y. Jiang, M. He and P. Wu, *J. Catal.*, 2007, **246**, 205.